

NATIONAL AERONAUTICS AND SPACE ADMINISTRATION

Technical Memorandum 33-563

*Measurements of the Structure of an Ionizing Shock
Wave in a Hydrogen-Helium Mixture*

Lewis P. Leibowitz

(NASA-CR-128343) MEASUREMENTS OF THE
STRUCTURE OF AN IONIZING SHOCK WAVE IN A
HYDROGEN-HELIUM MIXTURE L.P. Leibowitz
(Jet Propulsion Lab.) 1 Sep. 1972 17 p

N72-33265

Unclas

CSSL 20D G3/12

44062

**JET PROPULSION LABORATORY
CALIFORNIA INSTITUTE OF TECHNOLOGY
PASADENA, CALIFORNIA**

September 1, 1972



PRECEDING PAGE BLANK NOT FILMED

PREFACE

The work described in this report was performed by the Engineering Mechanics Division of the Jet Propulsion Laboratory.

ACKNOWLEDGMENT

The assistance of Clarence Tuttle in the performance of the experimental investigation, and the operation of the experimental facilities by Robert Chapman, are gratefully acknowledged.

CONTENTS

I.	Introduction	1
II.	Experiment	2
III.	Description of Analysis	3
	A. Reaction Scheme and Rate Equations	3
	B. Electron Temperature Equation	3
	C. Fluid Mechanics Equations	4
	D. Continuum Intensity Calculation	5
	E. Results of the Ionization Rate Calculations	5
IV.	Comparison of Experimental and Calculated Results	7
V.	Discussion and Conclusions	8
	References	9

TABLES

1.	Reaction scheme	11
2.	Rate constant expressions	12
3.	Cross section slope at threshold for excitation by atom-atom and electron-atom collisions of monatomic gases	13

FIGURES

1.	Schematic diagram of experimental apparatus	14
2.	Emission intensity measurements for a shock velocity = 15.0 km/sec and initial pressure = 267 N/m ² (2.0 torr)	14
3.	Calculated variation of concentrations and temperature with time behind a shock wave with shock velocity = 15.5 km/sec and initial pressure = 133 N/m ² (1.0 torr)	14
4.	A measured continuum intensity-time history is compared with calculations using a range of values for the atom-atom rate constant	14
5.	The effect of variations in k_3 on the calculated continuum intensity-time history	15
6.	Comparison of a calculated and measured intensity-time history for a run with slower shock velocity	15
7.	Experimentally obtained normalized ionization time compared with calculations	15
8.	Cross section for the excitation of hydrogen by electron-atom collisions	15
9.	Normalized ionization distance measurements of Belozarov and Measures, compared with the results of the present analysis, using the rate constant expressions of Table 2	16

ABSTRACT

Shock structure during ionization of a hydrogen-helium mixture has been followed using hydrogen line and continuum emission measurements. A reaction scheme is proposed which includes hydrogen dissociation and a two-step excitation-ionization mechanism for hydrogen ionization by atom-atom and atom-electron collisions. Agreement has been achieved between numerical calculations and measurements of emission intensity as a function of time for shock velocities from 13 to 20 km/sec in a 0.208 H₂ - 0.792 He mixture. The electron temperature was found to be significantly different from the heavy particle temperature during much of the ionization process. Similar time-histories for H β and continuum emission indicate upper level populations of hydrogen in equilibrium with the electron concentration during the relaxation process. The expression for the rate constant for excitation of hydrogen by atom-atom collisions that best fit the data was

$$k_{AA} = 4.0 \times 10^{-17} \left(\frac{8kT}{\pi\mu} \right)^{1/2} \exp(-10/kT) \text{ cm}^3 \text{ sec}^{-1},$$

where it has been assumed that the excitation cross section is the same for hydrogen and helium collision partners. The electron-atom excitation rate constant,

$$k_3 = 7.5 \times 10^{-16} \left(\frac{8kT_e}{\pi\mu_e} \right)^{1/2} \exp(-10/kT_e) \text{ cm}^3 \text{ sec}^{-1},$$

determined from this investigation, was in agreement with recent electron beam cross section measurements.

I. INTRODUCTION

While shock structure during ionization relaxation has been a subject of recent research for air, the noble gases, and alkali-metal vapors, the knowledge of hydrogen ionization relaxation is limited. An understanding of shock structure in hydrogen-helium mixtures is needed to determine the importance of nonequilibrium flow during atmospheric entry of probes to the outer planets. The presence of a thick nonequilibrium layer in the entry body flow-field could result in a significant reduction in the estimated radiative heating that the probe must be designed to withstand. In the present study, shock tube measurements and numerical analysis have been performed in order to understand the ionization and thermal processes which govern the shock structure in hydrogen-helium mixtures.

Much of the knowledge of collision processes governing the ionization of monatomic gases has come from studies of argon ionization by Petschek and Byron (Ref. 1), Harwell and Jahn (Ref. 2), Kelly (Ref. 3), Wong and Bershader (Ref. 4), Hoffert and Lien (Ref. 5), and others. Argon ionization is initiated by the excitation of argon atoms by atom-atom collisions. The excited atoms are then quickly ionized due to subsequent collisions. After a minimum number of electrons have been produced by atom-atom processes, the ionization is governed by a two-step electron-atom collision process. Good agreement has been obtained between experimental data and calculations based on this reaction scheme, assuming the existence of a separate electron and heavy particle temperature. The electron temperature was

found to be coupled to the ionization relaxation because ionization by electron-atom collisions was the dominant form of electron energy transfer.

The ionization and thermal processes governing shock structure in hydrogen-helium mixtures have been postulated (Ref. 6) based on the results of the investigations of argon. A reaction scheme is proposed which includes hydrogen dissociation, electronic excitation, and ionization by atom-atom and atom-electron collisions. Numerical solutions are obtained for the variation of fluid variables and species concentrations behind strong shock waves where the electron temperature has been allowed to differ from the heavy particle temperature during the relaxation process.

Ionization relaxation has been followed using spectroscopic emission measurements in a conical driver electric arc shock tube. Hydrogen line and continuum emission intensities were obtained as a function of time behind the incident shock wave in a 0.2079 H₂ - 0.7921 He mixture. This mixture allowed temperatures of interest to be achieved within the performance limits of the shock tube. From the agreement of calculated emission intensity time histories with the experimental data, it was inferred that a model describing the important processes governing shock structure had been obtained. New estimates of the rate constant for the excitation of hydrogen by atom-atom collisions were obtained and the rate constant for excitation of hydrogen by electron-atom collisions was found to be in agreement with electron beam cross section measurements.

II. EXPERIMENT

The time history of hydrogen line and continuum emission has been measured behind the incident shock wave in a mixture of hydrogen and helium. The effect on radiation relaxation rate of variations in shock velocity between 13 and 20 km/sec and of initial pressures between 33.3 and 267 N/m² (0.25 and 2.0 torr) has been determined. Shock waves were studied in a 0.152-m-diameter shock tube using the recently developed conical electric arc driver described by Menard (Ref. 7). Helium driver gas behind a thin aluminum diaphragm is heated and accelerated by the arc discharge of a 290-kilojoule capacitor bank.

Emission measurements were made of the H β line and the hydrogen continuum using a Jarrell Ash, 0.75-m, grating spectrometer. The spectral interval of the continuum channel was selected to avoid contributions from strong driver gas radiators. Channels were also selected to observe radiation from a helium line, a portion of a hydrogen molecular band, and a line of chromium which is a major radiator in the driver gas. The spectral intervals of each channel and a schematic drawing of the instrumentation are shown in Fig. 1. The photomultipliers (RCA 1P28A) and electronics had a combined response time of less than 0.2 μ sec. The time resolution of the optical system was less than the photomultiplier response time for the shock velocities studied in this investigation.

Arrival of the shock wave at the spectrometer station was detected with a Kistler pressure transducer, and shock velocities were measured using a series of photomultipliers and thin film resistance gages. The test gas used was a Matheson Gas mixture of 20.79% hydrogen with the balance helium. The mixture was prepared using ultra-high-purity grade gases and analyzed to have less than 2 ppm water, 0.5 ppm hydrocarbons, and 6 ppm nitrogen. Before each run the shock tube was evacuated to a pressure of at least 1.33×10^{-3} N/m² (1×10^{-5} mm Hg). The apparent leak rate was typically 4.4×10^{-4} N/m²-sec (2×10^{-4} torr/min). After evacuation the test

gas was continuously flushed through the shock tube for 2 min at the desired fill pressure.

Shock tube runs were made over the range of shock velocities from 13 to 20 km/sec and for initial pressures of 33, 133, and 267 N/m² (0.25, 1.0, and 2.0 torr). A sample of the data obtained from a run with 15.0 km/sec shock velocity is shown in Fig. 2. The slope of the signals from both the H β and hydrogen continuum channel ($\lambda = 514.5$ nm) were zero immediately behind the shock wave, increased to a maximum value, and then returned to zero as the steady state signal levels were approached. A characteristic relaxation time for the continuum signal, t_{lab} , was defined as shown in Fig. 2 by the intersection of the maximum slope line and the steady state value. The relaxation time for the H β emission was equal to the continuum relaxation time within the measuring accuracy. Both t_{lab} and the time between shock arrival and the initial jump in the intensity signal (induction time) decreased with increasing shock velocity, although the induction time became a smaller fraction of t_{lab} at the larger shock velocities. For shock velocities greater than 17 km/sec, the Kistler gage was not able to resolve the arrival of the shock wave and the initial jump in the intensity signal was assumed to indicate shock arrival.

From the relative intensities and time variations of the He and H₂ band channels it was concluded that the hydrogen continuum was the dominant source of radiation in these spectral intervals. Thus the radiation in all channels observed was governed by the hydrogen ionization process with no detectable sign of H₂ dissociation. The signals from the chromium channel were similar to the continuum channel until the arrival of the contact surface, when the signal level would increase by a large factor. The sudden decrease in the H β intensity at the same time as the jump in the Cr channel indicates that a test slug free of driver gas contamination was formed in the shock tube. Test times were more than adequate for relaxation measurements over the range of conditions used, and slug lengths were found to be approximately the tube diameter.

III. DESCRIPTION OF ANALYSIS

A. Reaction Scheme and Rate Equations

The reaction scheme describing the important collisional processes in hydrogen-helium ionizing shock waves has been modeled after the results obtained from studies of argon ionization (Refs. 4-5). Reactions are included which dissociate the molecular hydrogen, excite the electronic states of hydrogen and helium, and ionize the hydrogen and helium by collisions with atoms and with electrons. Table 1 lists the 11 steps of the reaction scheme. Photo-ionization and precursor effects are considered negligible, consistent with the findings of Bates, Kingston, and McWhirter (Refs. 8 and 9).

Ionization of hydrogen is initiated by atom-atom collisions which produce atoms in electronically excited states that are subsequently ionized by additional collisions. A simplified model is assumed in which hydrogen in the first excited state is produced by collisions with hydrogen (reaction 5) and from collisions with helium (reaction 6). It is assumed that excitation to the $n = 2$ level is the rate-limiting step and the excited atoms are rapidly ionized by further collisions. Hydrogen ionization by electron-atom collisions also proceeds by a two-step excitation-ionization process in which the ionization of excited hydrogen is assumed to be rapid. The direct ionization of hydrogen by electron-atom collisions is included as reaction 1. Helium is ionized by collisions with electrons from a single step process in reaction 2 and by an excitation-ionization process in reaction 4.

The reaction scheme for the dissociation of hydrogen has been obtained from shock tube investigations (Refs. 10-14). Hydrogen is first dissociated by collisions with itself and helium; but, subsequently, it is dissociated by collisions with atomic hydrogen, ions, and electrons.

The knowledge of rate constants for hydrogen ionization is incomplete. No definitive estimates of atom-atom rate constants have been made. The rate constants for excitation and ionization by electron-atom collisions were calculated using data obtained from electron beam cross section measurements. A fit of the cross section data was obtained by matching the initial slopes of the cross section data and the expression $Q_i = \sigma_i (1 - E_{i,0}/E)$. Assuming a Maxwell-Boltzmann distribution of reactants, the resulting expression for the rate constants (Ref. 15) is

$$k_i = \sigma_i \left(\frac{8kT}{\pi\mu} \right)^{1/2} \exp(-E_{i,0}/kT),$$

where $E_{i,0}$ is the threshold energy for reaction (i), σ_i is an adjustable parameter, and μ is the reduced mass. Initial estimates of the rate constant for atom-atom excitation of hydrogen were made assuming that the ratio of the atom-atom and atom-electron excitation cross section for hydrogen was approximately the same as the ratio for the Noble gases (Ref. 16). The rate constant expressions used in this investigation are shown in Table 2.

Hydrogen dissociation reactions have been studied in shock-heated mixtures of argon and hydrogen over the range of temperatures $5000 > T > 2500^\circ$ by Myerson and Watt (Ref. 10), Jacobs, Giedt, and Cohen (Ref. 11), Patch (Ref. 12), Rink (Ref. 13), and Sutton (Ref. 14). The expressions for the rate constants given by Jacobs et al. were found to represent the best compromise of the experimental data obtained by all investigators and were suitable for extrapolation to temperatures greater than 5000°K . The rate constants for the hydrogen dissociation reaction with helium and with argon as collision partners were assumed to be equal.

The rate constants for the reverse direction of each reaction step were found, assuming the principle of detailed balancing. Thus, the reverse rate constant for a given step was equal to the rate constant for the forward direction divided by the equilibrium constant for that reaction. The equilibrium constants were obtained by fitting data produced by the thermochemistry program of Menard and Horton (Ref. 22) with the expressions

$$K_{\text{H}^+} = 4.05 \times 10^{-9} T^{3/2} \times \exp(-1.578 \times 10^5/T) \text{ mole/cm}^3,$$

$$K_{\text{He}^+} = 1.62 \times 10^{-8} T^{3/2} \times \exp(-2.853 \times 10^5/T) \text{ mole/cm}^3,$$

and

$$K_{\text{H}} = 3.7 [1.0 - \exp(-1.50 \times 10^8 T^{-2})] \times \exp\left(\frac{-52340}{T}\right) \text{ mole/cm}^3.$$

Six equations are needed to describe the concentrations of the species H_2 , H , H^+ , He , He^+ , and e in the present system. Reaction rate equations for H , e , and He^+ are used along with three conservation of atomic species relations. The concentrations of all species are found by simultaneously solving the differential equations, the conservation of atomic species relations, the fluid mechanics equations, and the electron energy equation.

B. Electron Temperature Equation

As a consequence of the large ratio of atom or ion mass to electron mass, electrons transfer energy rapidly by collisions with other electrons but only slowly by elastic collisions with atoms or ions. The number of collisions necessary to produce a Maxwellian velocity distribution between electrons and atoms is larger than the number of collisions necessary to produce a Maxwellian distribution among electrons by a factor of the mass ratio. Therefore, throughout an ionizing shock wave, separate Maxwellian distributions describe the populations of electrons and heavy particles

and thus, a different temperature is given to atoms and electrons in the same gas.

The electron temperature is obtained from the solution to the electron energy equation. The change in electron energy is the sum of the energy exchanged by elastic and inelastic collisions between electrons and heavy particles, where inelastic collisions are those which result in ionization of the heavy particles with resulting losses in electron energy. A discussion of the electron energy equation for a nonequilibrium gas is given by Appleton and Bray (Ref. 23). For a one-dimensional steady shock wave in a H₂-He mixture, the resulting equation is

$$\frac{\partial}{\partial y} (\epsilon_e u) = 3(e)m_e \bar{v} R(T - T_e) - \theta_H (R_1 - R_{1r} + R_3 - R_{3r}) - \theta_{He} (R_2 - R_{2r} + R_4 - R_{4r}) \quad (1)$$

where ϵ_e = energy per unit volume of the electron, which is given by

$$\epsilon_e = \frac{3}{2}(e)RT_e,$$

y = distance behind the shock wave,

(e) = concentration of electrons,

m_k = mass of species k ,

ν_{ek} = collision frequency for elastic collisions between electrons and species k ,

θ_k = ionization energy per mole of species k ,

$$\bar{v} = \sum_k \nu_{ek}/m_k,$$

and the (R_i) 's are the forward and reverse reaction rates for electron production. Equation (1) can be simplified using the steady-state approximation, thereby setting the right-hand side of Eq. (1) equal to zero. This corresponds to the case where the energy is used by the electrons for ionization at the same rate that it is received from elastic collisions and has been discussed by Petschek and Byron (Ref. 1) and Hoffert and Lien (Ref. 5). The steady-state approximation results in the following relation for electron temperature:

$$T_e = T - \frac{\theta_H(R_1 - R_{1r} + R_3 - R_{3r}) + \theta_{He}(R_2 - R_{2r} + R_4 - R_{4r})}{3m_e n_e \bar{v}} \quad (2)$$

where the reaction rates are strong functions of T_e due to the exponential dependence of the rate constants. An explicit equation for T_e suitable for numerical solution can be obtained by approximating the rate constants by linear functions of T_e for each integration step. Using the expressions

$$k_H = k_1 + k_3 = a_H T_e + b_H,$$

and

$$k_{He} = k_2 + k_4 = a_{He} T_e + b_{He},$$

Eq. (2) becomes

$$T_e = \frac{T - \frac{1}{3m_e \bar{v}} b_H \theta_H(H) + b_{He} \theta_{He}(He) - R_r}{1 + \frac{1}{3m_e \bar{v}} a_H \theta_H(H) + a_{He} \theta_{He}(He)} \quad (3)$$

where

$$R_r = \theta_H(R_{1r} + R_{3r})/n_e + \theta_{He}(R_{2r} + R_{4r})/n_e.$$

The elastic collision frequency can be written in terms of the elastic collision cross section using the approximate expression

$$\nu_{ek} = n_k v_e Q_{ek}$$

where

n_k = molar concentration of species k ,

v_e = average electron velocity given by

$$v_e = \left(8kT_e/\pi m_e\right)^{1/2},$$

and

Q_{ek} = the elastic collision cross section for species k .

The cross sections for electron-neutral collisions were obtained by fitting experimentally measured data with expressions of the form

$$Q_{ek} = A_k \exp(-aE) - \exp(-bE).$$

The coefficients used are as follows: for He using data from Gould and Brown (Ref. 24), $A = 7.85 \times 10^{-16}$, $a = 0.20$, and $b = 4.0$; for H₂ using data from Brode (Ref. 25), $A = 2.80 \times 10^{-15}$, $a = 0.3330$, and $b = 2.0$; and for H using data from Brackmann, Fite, and Neynaber (Ref. 26), $A = 3.95 \times 10^{-15}$, $a = 0.589$, and $b = \infty$. The Coulomb cross section given by the expression

$$Q_{eH^+} = 1.95 \times 10^{-6} T_e^{-2.0} \ln(1.53 \times 10^8 T_e^3/n_e) (\text{cm}^2)$$

was used for H⁺ and He⁺.

C. Fluid Mechanics Equations

The fluid mechanics of a one-dimensional shock wave with constant incident flow velocity is described, in a coordinate system fixed to the shock wave, by the continuity equation,

$$\rho_1 u_1 = \rho_2 u_2, \quad (4)$$

the momentum equation,

$$p_1 + \rho_1 u_1^2 = p_2 + \rho_2 u_2^2, \quad (5)$$

the energy equations,

$$h_1 + \frac{u_1^2}{2} = h_2 + \frac{u_2^2}{2}, \quad (6)$$

and the equations of state where the subscript (1) represents conditions in front of the shock wave, subscript (2) represents conditions behind the shock wave, and ρ , u , and h are the mass density, fluid velocity, pressure, and enthalpy per unit mass respectively. For a multicomponent, chemically reacting gas with the electrons described by a separate temperature T_e , the equations of state are

$$p = \rho RT \sum_i \frac{Y_i}{W_i} + n_e RT_e \quad (7)$$

and

$$h = \sum_i^{n-1} Y_i (h_i^f + c_{p_i} T) + Y_e c_{p_e} T_e \quad (8)$$

where W_i is the molecular weight of species i and $Y_i = \rho_i/\rho$ is the mass fraction of species i , h_i^f is the heat of formation per unit mass of species i , and c_{p_i} is the specific heat per unit mass of species i .

The value of the species concentrations are given by the relation

$$\frac{d}{dt} (n_i/\rho) = R_i/\rho \quad (9)$$

where t is the particle time and R_i is the chemical production rate of species i . It is not necessary to solve a rate equation for each species present in the system. An equation for the conservation of atomic element may be written for each element present in the system. In terms of the frozen conditions, the conservation of atomic elements relation becomes

$$\sum_i \alpha_{ij} n_i/\rho = \sum_i \alpha_{ij} n_i^0/\rho^0, \quad (10)$$

where α_{ij} = number of atoms of element j per species i and $(^0)$ represents the frozen conditions in front of the shock wave.

An explicit relation for the density ratio as a function of species mass fraction and T_e is obtained by combining the conservation equations:

$$\frac{\rho_1}{\rho_2} = \frac{-B - (B^2 - 4AC)^{1/2}}{2A} \quad (11)$$

where

$$A = \frac{\gamma}{2} M^2 (2\Gamma - 1),$$

$$B = -\Gamma(1 + \gamma M^2 - n_e RT_e/\rho_1),$$

$$C = \Gamma^0 + \gamma M^2/2 - \frac{\gamma}{2} \sum_i^{n-1} (Y_i - Y_i^0) h_i^f$$

$$- \gamma Y_e c_{p_e} T_e/a_1^2,$$

$$\Gamma = \frac{\overline{wc}}{R} = \frac{\sum_i^{n-1} Y_i c_{p_i}}{R \sum_i^{n-1} Y_i/W_i}$$

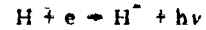
M is the Mach number, a is the incident speed of sound, γ is the average specific heat, and the superscript $(^0)$ represents the frozen conditions in front of the shock wave.

D. Continuum Intensity Calculation

The continuum emission intensity during ionization relaxation is a function of electron concentration, temperature, and the established radiative cross sections for hydrogen. Radiative processes that contribute to hydrogen continuum emission are radiative recombination



and radiative attachment of hydrogen



for temperatures below 15,000°K.

For an optically thin gas emission, intensity is given by the expression

$$S_\lambda = B_\lambda (\sigma_H n_e^2 + \sigma_{H^-} K_{H^-} n_{H^-} n_e) l,$$

where S_λ is the specific intensity in watt $\text{cm}^{-3} \text{ster}^{-1}$, B_λ is the Planck function, σ_H is the radiative recombination cross section, σ_{H^-} is the negative hydrogen ion absorption cross section, l = path length, K_{H^-} is the equilibrium constant for H^- , n_e is the number density of electrons, and n_{H^-} is the number density of hydrogen atoms. Empirical relations used for the cross sections at $\lambda = 514.5 \text{ nm}$ were

$$\sigma_H = (1.208 \times 10^{-38} - 1.98 \times 10^{-43} T_e) \times \exp(2.865 \times 10^4/T_e) \text{ cm}^2$$

obtained from a fit to the absorption coefficients calculated by Stickford (Ref. 27) and

$$\sigma_{H^-} = 2.21 \times 10^{-17} + 1.07 \times 10^{-21} T_e \text{ cm}^2$$

obtained from a fit of the data presented by Griem (Ref. 28). The assumption has been made that H^- is in local equilibrium with the electron concentration during the course of the reaction. This is justified by the fact that the formation time for H^- is small compared with the ionization time.

E. Results of the Ionization Rate Calculations

The variation of species concentrations, temperature, and emission intensity as a function of time have been obtained from numerical solutions to Eqs. (3), (9), (10), and (11). The chemical rate equations were solved using a Runge-Kutta integration scheme with separate step size for the dissociation and ionization regions. In Fig. 3 the variation in properties behind a shock wave are shown for a velocity of 15.5 km/sec in a 0.208 H_2 - 0.792 He mixture. The dissociation of H_2 is completed before appreciable ionization can take place. The increase in H concentration with time is due to the increase in total density during ionization, which offsets the removal of H atoms by ionization. The shape of the electron concentration curve is similar to that obtained during argon ionization. Initially electrons are produced

primarily by Reactions 5 and 6. As the electron concentration and temperature increase, the rate of Reaction 3 increases until it becomes the dominant electron producer. The arrow in Fig. 3 denotes the point where the reaction rate for Reaction 3 equals the rate for Reactions 5 and 6. Reactions 1, 2, and 4 were found to be unimportant under the conditions of this investigation but have been included for completeness.

The electron temperature differs from the heavy particle temperature during the ionization relaxation. The initial drop in temperature is due to dissociation of H_2 and is then followed by a slow increase in temperature during the early stages of ionization. During the later stages of ionization, the electron temperature asymptotically approaches the heavy particle temperature. The deviation between the electron and heavy particle temperature was found to be proportional to the temperature behind the shock wave and therefore the shock velocity. Results using the steady state treatment for the electron energy equation have been checked with exact numerical solutions of the electron energy equation, including a term for the energy of the electrons produced by atom-

atom collisions. The steady state solution and the exact solution were found to converge within a time that was much shorter than the dissociation time. The atom-atom term and the initial value of T_e were found to have negligible effect on the solution a small distance behind the shock wave. This is consistent with estimates of the relative importance of the atom-atom term using simplified analysis.

The significant difference found between T_e and T during the ionization process is in disagreement with the results of Belozarov and Measures (Ref. 29). Their analysis indicated that the electron temperature in hydrogen closely followed the heavy particle temperature throughout the relaxation region and concluded that this was due to a large cross section for elastic H-e collisions. Their expression for the rate of energy transfer by elastic collisions contains an incorrect integral of the cross section which overestimates the correct value by a factor of 40. Electron temperature profiles in agreement with Belozarov and Measures can be produced using the expression $40 Q_{eH}$ in the present analysis.

IV. COMPARISON OF EXPERIMENTAL AND CALCULATED RESULTS

Comparisons have been made between experimental measurements and computer calculations of the continuum intensity as a function of time. Important rate constants were varied in order to obtain a best fit with the experimental data and also to determine the sensitivity of the results to changes in each of the rate constants. From the agreement of the calculation with the experimental data values for the atom-atom and atom-electron excitation rate, constants were obtained within the factor of uncertainty of the data. The reactions which govern the ionization process are the atom-atom reactions (Reactions 5 and 6) and the atom-electron excitation reaction (Reaction 3), while the direct ionization reactions were found to play a negligible role. In this investigation the assumption has been made that the collision cross sections for electron excitation of hydrogen by H-H and H-He collisions are identical. Thus the rate constants for Reactions 5 and 6 are identical, except for the reduced mass, and will be referred to as k_{AA} .

In Figs. 4 and 5 the effects of the atom-atom and electron-atom rate constants on the calculated continuum intensity are shown. The experimental emission intensity signal shown in Figs. 4 and 5 has been normalized to the calculated equilibrium value. As can be expected, the atom-atom rate constant affects only the early stage of the reaction. In Fig. 4 it is seen that an increase of the atom-atom rate constants has little effect on the maximum slope of the intensity-time history but causes a steady decrease in the induction time (the intersection of the maximum slope line with the abscissa). A best fit to the emission intensity signal is obtained for a value of the atom-atom rate constant of

$$k_{AA} = 4.0 \times 10^{-17} \left(\frac{8kT}{\pi\mu} \right)^{1/2} \exp(-10.0/kT) \text{ cm}^3 \text{ sec}^{-1} \quad (12)$$

Using the values $0.25 k_{AA}$ and $4 k_{AA}$ causes the calculated emission intensity to fall outside of the range of uncertainty of the experimental measurements. This is an indication of the sensitivity of the calculations to changes in the atom-atom rate constants.

The effect on the calculations of variations of the electron-atom rate constant k_3 is shown in Fig. 5. The value for k_3 was varied over the range of uncertainty in the electron beam measurement of electron-atom excitation cross sections while keeping the value of all other rate constants fixed. The maximum slope of the emission intensity and therefore the relaxation time was directly

affected by the value of k_3 , while the induction time was insensitive to changes in k_3 . The expression for k_3 obtained from the cross-section measurements,

$$k_3 = 7.5 \times 10^{-16} \left(\frac{8kT_e}{\pi\mu_e} \right)^{1/2} \exp(-10.0/kT_e) \text{ cm}^3 \text{ sec}^{-1}, \quad (13)$$

was found to give the best agreement with the emission intensity measurements. Due to the sensitivity of k_{AA} to the induction time and k_3 to the maximum slope, it was possible to unambiguously determine the expressions for each rate constant which best fit the experimental data. A comparison of a measured and calculated emission intensity time history for another set of conditions, $U_1 = 13.7 \text{ km/sec}$ and $p_1 = 267 \text{ N/m}^2$, is shown in Fig. 6.

The dependence of experimental and calculated relaxation data on shock velocity and initial pressure has been investigated. A characteristic time for ionization in the shock fixed coordinate system, τ_{ion} , was defined as the product of the density ratio across the shock wave and t_{lab} . In Fig. 7, experimental values of $(H_2)_2 \tau_{ion}$ are shown as a function of $1/T_{2,0}$, where $(H_2)_2$ is the H_2 concentration immediately behind the shock wave and $T_{2,0}$ is the corresponding temperature. Also shown in Fig. 7 are calculated values of $(H_2)_2 \tau_{ion}$ for a range of values of k_{AA} . The calculations are in good agreement with the experimental data using the expression for k_{AA} given in Eq. (12). The small dependence on p_1 indicated by the calculated results was within the scatter of the data and could not be experimentally verified. Calculated results using $0.25 k_{AA}$ and $4.0 k_{AA}$, shown in Fig. 7, bracket the experimental data and give upper and lower limits on the uncertainty in the determination of k_{AA} . The error bars shown in Fig. 7 are indications of the experimental uncertainties in the determination of ionization time and the temperature. The largest uncertainty in τ_{ion} occurs at the smaller values of $1/T_{2,0}$ due to the approach of rise time limitations on the measurement of shock wave arrival time and radiation relaxation rate. For the slower shock velocities, the principal uncertainty in τ_{ion} is due to oscillogram reading errors caused by the decrease in signal-to-noise ratio. The uncertainties in the values for $1/T_{2,0}$ are caused by limitations on the accuracy of the shock velocity measurement and are largest at the lower shock velocities due to the increasing rate of change of $1/T_{2,0}$ with decreasing U_1 .

V. DISCUSSION AND CONCLUSIONS

A model has been proposed for ionization processes governing shock structure in hydrogen-helium mixtures, and experimental data have been obtained which match the predictions of the model. The dissociation of hydrogen takes place in a region behind the shock wave that is small compared with ionization. The ionization process is governed by two separate regions: one dominated by the excitation of atomic hydrogen due to atom-atom collisions and the second due to hydrogen excitation by collisions with electrons. The electron temperature was found to be significantly different from the heavy particle temperature during the early portion of the reaction but equaled the heavy particle temperature during the later part of the reaction.

Data obtained on the relaxation time for the H β signal is consistent with the postulated reaction model. The H β relaxation times and the continuum relaxation times were found to be equal within the accuracy of the data. It was concluded from these results that the population of the $n = 4$ level of hydrogen follows the electron concentration. This is consistent with the reaction mechanism which assumes that all excited levels of hydrogen are in quasi-equilibrium with the electron concentration and the excitation of the first excited state is the rate limiting step.

The agreement of the calculation with experimental emission measurements has produced estimates of the rate constants for the excitation of hydrogen to its first excited state by collisions with hydrogen and helium. The ratio of the cross section for hydrogen excitation by atom-atom collisions to the cross section for excitation by atom-electron collisions was found to be 5.34×10^{-2} . The cross section data are compared with data for other monatomic gases in Table 3, where values of S , the slope of the cross section curve at threshold, are shown for each species. It can be seen that while both the atom-atom and atom-electron excitation cross sections for hydrogen are considerably larger than those for the other gases, the ratio of atom-atom to atom-electron cross sections falls between the values for argon and krypton. The rate constant for atom-atom excitation of hydrogen was found to be on the order of 500 times larger than that of argon, which is consistent with the finding the hydrogen-bearing impurities have a strong effect on argon ionization time measurements.

The expression for k_3 that fits the data from this investigation is consistent with recent electron beam cross section measurements of hydrogen excitation. The rate constant expression for k_3 given by Eq. (13) was obtained by combining

the cross section data for excitation of the 2p level of McGowan, Williams, and Curley (Ref. 19) and the data for the excitation of the 2s level by Kauppila, Ott, and Fite (Ref. 20). This combined cross section is shown in Fig. 8 along with the combined cross section obtained using the McGowan et al. data and the 2s data of Lichten and Schultz (Ref. 31). Both curves for the combined cross section are seen to have the same initial slope. Error bars are used to show the experimental uncertainty in the measurements. Variations in the initial slope of the cross section analogous to the range of k_3 considered in Fig. 5 are shown in Fig. 8. The upper cross section slope indicates the experimental uncertainty of the electron beam. The lower cross section slope was obtained using values from the earlier measurements of Fite, Stebbings, and Brackmann (Ref. 32), and Stebbings, Fite, Hummer, and Brackmann (Ref. 33). From Fig. 5, it can be seen that the sensitivity of the shock tube measurements for determining the excitation cross section is at least as good as the beam measurements. Thus shock tube data can be useful in obtaining cross section slopes at the threshold to supplement the data obtained from beam experiments.

No results of ionization time measurements for hydrogen-helium mixtures have been previously published. Studies of ionization rates in hydrogen or hydrogen-helium mixture using diaphragmless electromagnetic shock-tubes have been made by Nakagawa and Wisler (Ref. 34), Wisler (Ref. 35), Fukuda, Okasaka, and Fujimoto (Ref. 36), and Belozarov and Measures (Ref. 29). Only Belozarov and Measures were able to produce flow behind the shock wave that was thought to be free of driver gas mixing. Their results for the normalized ionization distance in hydrogen are shown in Fig. 9 along with results using the present analysis. The ionization distances calculated using the expression for k_{AA} from the present investigation are considerably larger than the measurements. However, calculated results using $5.0 k_{AA}$ give good agreement with the results of Belozarov and Measures. This value of k_{AA} agrees with the present investigation if it is assumed that initial excitation of hydrogen occurs only by H-H collisions and that Reaction 6 is unimportant. It was assumed in this study that the cross section for excitation was the same for both collision partners. At the present time there is no theoretical or experimental evidence to indicate that the excitation of hydrogen is much more probable by collisions with hydrogen atoms than by helium atoms. Subsequent studies of relaxation rates for a range of hydrogen-helium mixtures will be undertaken to determine the relative efficiency of these collision partners.

REFERENCES

1. Petschek, H., and Byron, S., Annals of Physics 1, 270 (1957).
2. Harwell, K., and Jahn, R., Phys. of Fluids 7, 214 (1964).
3. Kelly, A. J., J. Chem. Phys. 45, 1723 (1966).
4. Wong, H., and Bershader, D., J. Fluid Mech. 26, 459 (1966).
5. Hoffert, M., and Lien, H., Phys. of Fluids 10, 1769 (1967).
6. Leibowitz, L. P., Bull. Am. Phys. Soc. 16, 1320 (1971).
7. Menard, W. A., AIAA J. 9, 2096 (1971).
8. Bates, D. R., Kingston, A. E., and McWhirter, R. W. P., Proc. Roy. Soc. (London) 267A, 297 (1962).
9. Bates, D. R., Kingston, A. E., and McWhirter, R. W. P., Proc. Roy. Soc. (London) 270A, 155 (1962).
10. Myerson, A. L., and Watt, W. J., J. Chem. Phys. 49, 425 (1968).
11. Jacobs, T., Giedt, R., and Cohen, N. J., J. Chem. Phys. 47, 54 (1967).
12. Patch, R. W., J. Chem. Phys. 36, 1919 (1962).
13. Rink, J., J. Chem. Phys. 36, 262 (1962).
14. Sutton, E. A., J. Chem. Phys. 36, 2923 (1962).
15. Ross, J., Light, J., and Schuler, K., Kinetic Processes in Gases and Plasmas, Edited by A. Hochstern, Academic Press, N. Y. (1969).
16. Merito, M., and Morgan, E., J. Chem. Phys. 52, 2192 (1970).
17. Fite, W., and Brackmann, R., Phys. Rev. 112, 1141 (1958).
18. Massey, H., and Burhop, E., Electronic and Ionic Impact Phenomena, Oxford Press, Oxford (1952).
19. McGowan, J. W., Williams, J. F., and Curley, E. K., Phys. Rev. 180, 132 (1969).
20. Kauppila, W. E., Ott, W. R., and Fite, W. L., Phys. Rev. A1, 1099 (1970).
21. Holt, H., and Krotkov, R., Phys. Rev. 144, 144 (1966).
22. Horton, T., and Menard, W., TR 32-1350, Jet Propulsion Laboratory, Pasadena, California (1960).
23. Appleton, J. P., and Bray, K. N. C., J. Fluid Mech. 20, 659 (1964).
24. Gould, L., and Brown, S. C., Phys. Rev. 95, 897 (1954).
25. Brode, R. B., Rev. Modern Phys. 5, 257 (1933).
26. Brackmann, R. T., Fite, W. L., and Neynaber, R. H., Phys. Rev. 112, 1157 (1958).
27. Stickford, G., J. Quant. Spectry, Radiative Transfer 12, 525 (1972).
28. Griem, H. R., Plasma Spectroscopy, McGraw-Hill, New York 537 (1964).
29. Belozarov, A. N., and Measures, R. M., J. Fluid Mech. 36, 695 (1969).
30. Kaha, S. P., and Measures, R. M., Phys. of Fluids 14, 2544 (1971).
31. Lichten, W., and Schultz, S., Phys. Rev. 116, 1132 (1959).

REFERENCES (contd)

32. Fite, W. L., Stebbings, R. F., and Brackmann, R. T., Phys. Rev. 116, 356 (1959).
33. Stebbings, R. F., Fite, W. L., Hummer, D. G., and Brackmann, R. T., Phys. Rev. 119 (1960)
34. Nakagawa, Y., and Wisler, D., Seventh International Shock Tube Symp., Toronto, 622 (1969).
35. Wisler, D., Ph.D. Thesis, University of Colorado (1970).
36. Fukuda, K., Okasaka, R., and Fujimoto, T., Seventh International Shock Tube Symp., Toronto 446 (1969).

Table 1. Reaction scheme

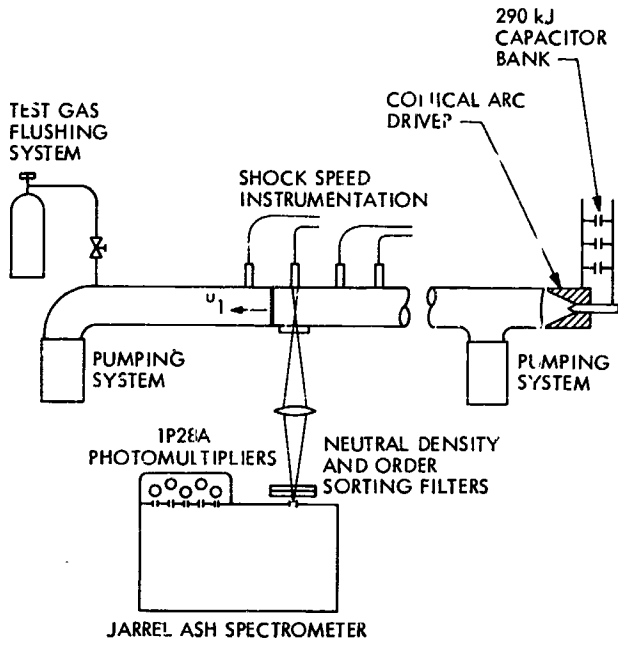
1.	$H + e$	\rightleftharpoons	$H^+ + e + e$
2.	$He + e$	\rightleftharpoons	$He^+ + e + e$
3.	$H + e$	\rightleftharpoons	$H^* + e$
4.	$He + e$	\rightleftharpoons	$He^* + e$
5.	$H + H$	\rightleftharpoons	$H^* + H$
6.	$H + He$	\rightleftharpoons	$H^* + He$
7.	$H_2 + He$	\rightleftharpoons	$H + H + He$
8.	$H_2 + H_2$	\rightleftharpoons	$H + H + H_2$
9.	$H_2 + H$	\rightleftharpoons	$H + H + H$
10.	$H_2 + H^+$	\rightleftharpoons	$H + H + H^+$
11.	$H_2 + e$	\rightleftharpoons	$H + H + e$

Table 2. Rate constant expressions

Reaction	Rate constants in $\text{cm}^3 \text{sec}^{-1}$	Reference
1	$k_1 = 6.09 \times 10^{-17} \left(\frac{8kT_e}{\pi\mu_e} \right)^{1/2} \exp(-13.6/kT_e)$	17
2	$k_2 = 3.56 \times 10^{-17} \left(\frac{8kT_e}{\pi\mu_e} \right)^{1/2} \exp(-24.58/kT_e)$	18
3	$k_3 = 7.5 \times 10^{-16} \left(\frac{8kT_e}{\pi\mu_e} \right)^{1/2} \exp(-10/kT_e)$	19, 20
4	$k_4 = 6.00 \times 10^{-17} \left(\frac{8kT_e}{\pi\mu_e} \right)^{1/2} \exp(-20/kT_e)$	21
5	$k_5 = 4.0 \times 10^{-17} \left(\frac{8kT}{\pi\mu} \right)^{1/2} \exp(-10/kT)$	--
6	$k_6 = 4.0 \times 10^{-17} \left(\frac{8kT}{\pi\mu} \right)^{1/2} \exp(-10/kT)$	--
7	$k_7 = 6.93 \times 10^{-6} T^{-1} \exp(103240/RT)$	11
8	$k_8 = 2.5 k_7$	11
9	$k_9 = 20.0 k_7$	11
10	$k_{10} = k_9$	--
11	$k_{11} = k_9$	--

Table 3. Cross section slope at threshold for excitation by atom-atom and electron-atom collisions of monatomic gases

Gas	$S_{AA}, \text{cm}^2/\text{ev}$	$S_{eA}, \text{cm}^2/\text{ev}$	S_{AA}/S_{Ae}	Reference
H	4.0×10^{-18}	7.5×10^{-17}	5.34×10^{-2}	Present investigation
Ar	1.2×10^{-19}	4.9×10^{-18}	2.45×10^{-2}	3
Kr	1.4×10^{-19}	2.32×10^{-18}	6.0×10^{-2}	15
Xe	6.0×10^{-21}	3.80×10^{-18}	1.58×10^{-3}	15
He	2.0×10^{-19}	2.86×10^{-17}	7.0×10^{-3}	30



SPECTRAL INTERVALS

SPECIES	λ , nm	$\Delta\lambda$ nm
Cr	425.4	0.5
He	447.1	0.5
H ₂	462.8	1.0
H β	486.1	0.5
H ⁺ + e	514.5	1.0

Fig. 1. Schematic diagram of experimental apparatus

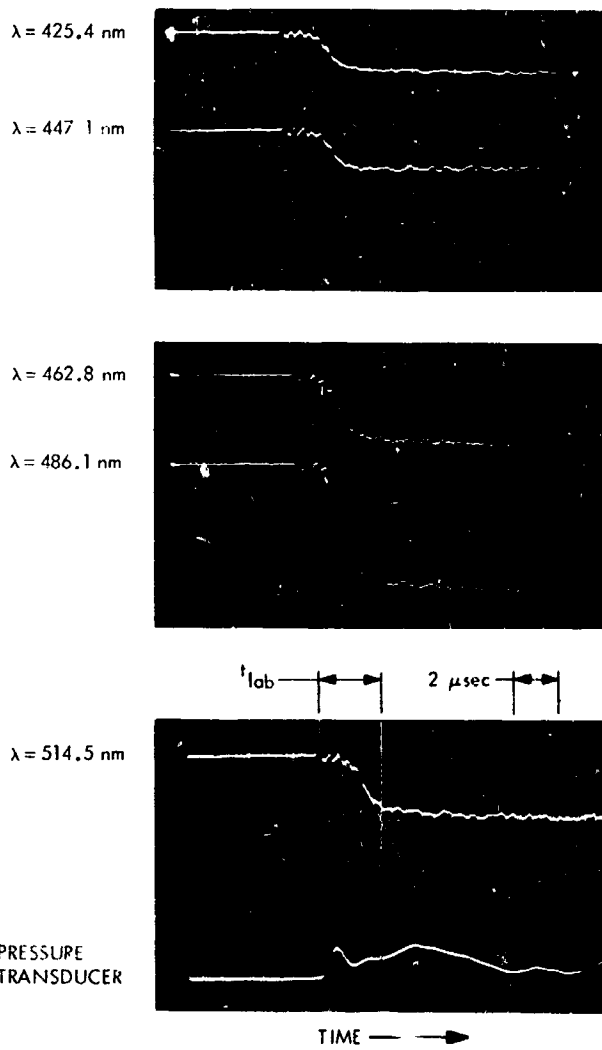


Fig. 2. Emission intensity measurements for a shock velocity = 15.0 km/sec and initial pressure = 267 N/m² (2.0 torr). The characteristic time for relaxation of the $\lambda = 514.5$ nm signal is defined.

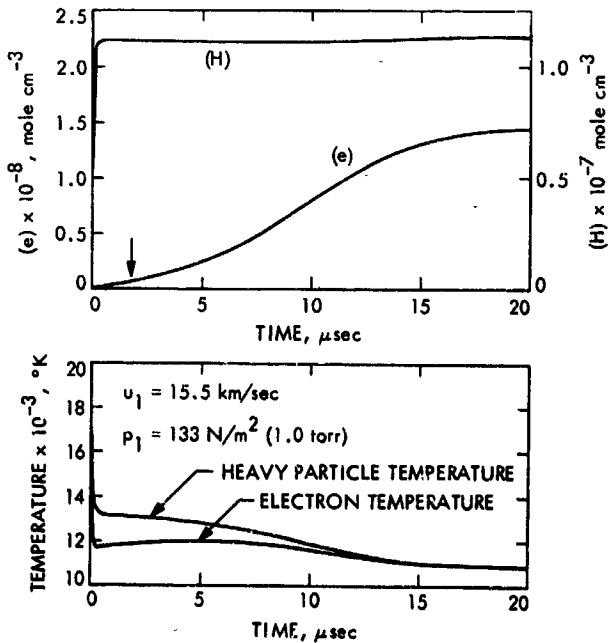


Fig. 3. Calculated variation of concentrations and temperature with time behind a shock wave with shock velocity = 15.5 km/sec and initial pressure = 133 N/m² (1.0 torr)

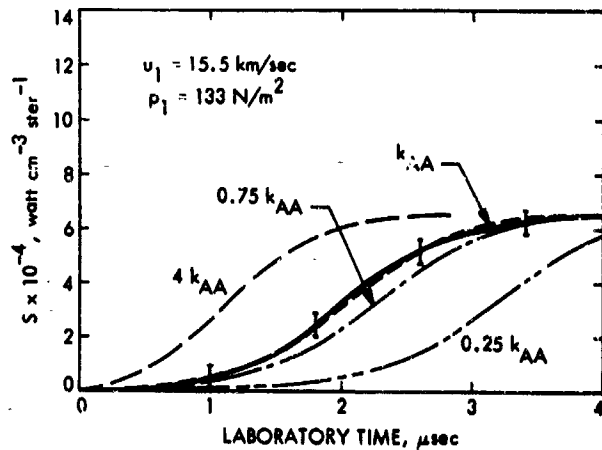


Fig. 4. A measured continuum intensity-time history is compared with calculations using a range of values for the atom-atom rate constant. The solid line represents the experimental data.

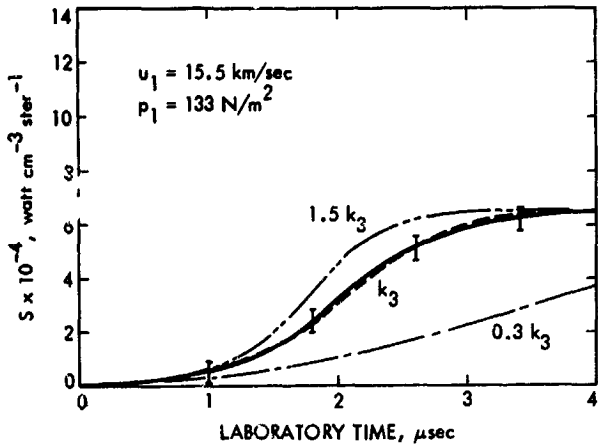


Fig. 5. The effect of variations in k_3 on the calculated continuum intensity-time history

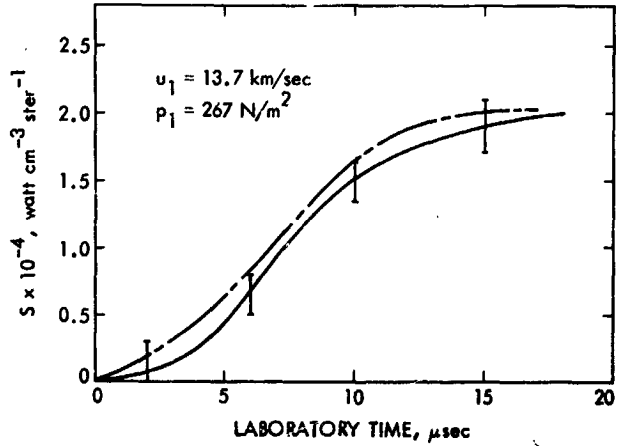


Fig. 6. Comparison of a calculated and measured intensity-time history for a run with slower shock velocity

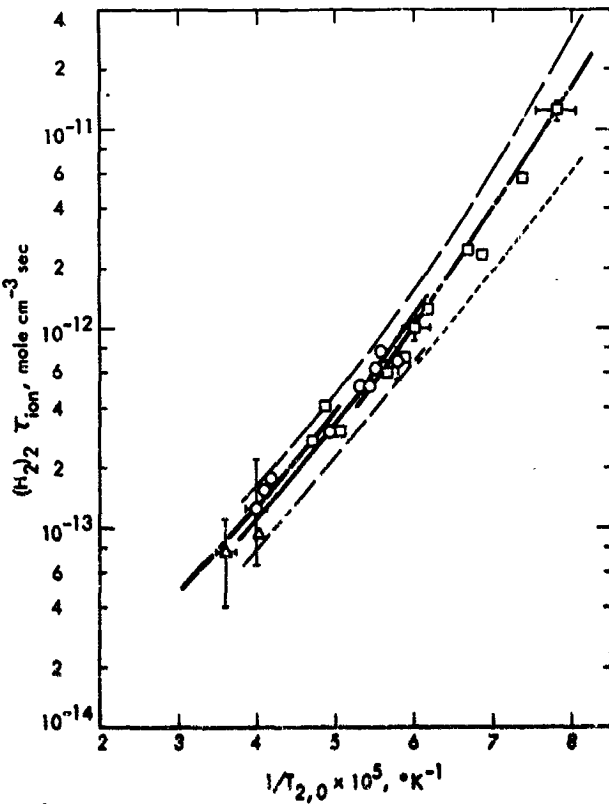


Fig. 7. Experimentally obtained normalized ionization time compared with calculations; Δ - $p_1 = 33.3 \text{ N/m}^2$, \circ - $p_1 = 133 \text{ N/m}^2$, \square - $p_1 = 267 \text{ N/m}^2$. The dark curves represent calculations using the rate constant expressions shown in Table 2 for, from left to right, $p_1 = 33.3, 133, \text{ and } 267 \text{ N/m}^2$. The dashed curves indicate the effect of a factor of 4 increase and decrease to k_{AA} .

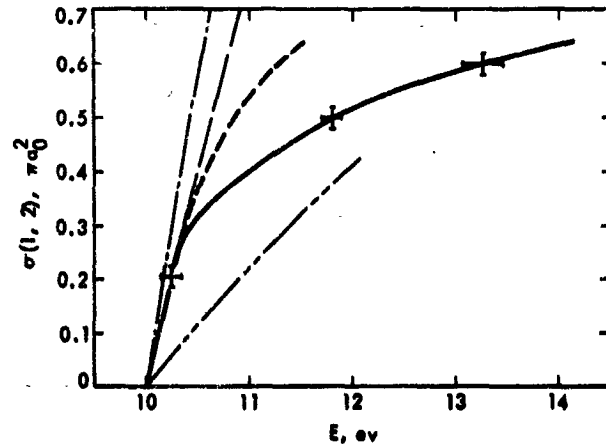


Fig. 8. Cross section for the excitation of hydrogen by electron-atom collisions where

- combined cross section from Refs. 19 and 20
- - - - - combined cross section from Refs. 19 and 30
- equivalent cross section for k_3
- · - · - equivalent cross section for $1.5 k_3$
- · — · — equivalent cross section for $0.3 k_3$

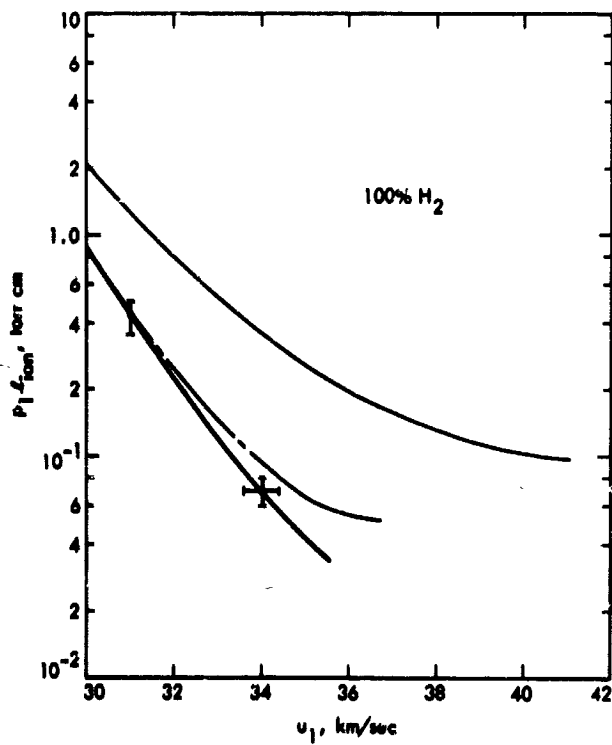


Fig. 9. Normalized ionization distance measurements of Belozarov and Measures, compared with the results of the present analysis using the rate constant expressions of Table 2, and $5.0 k_{AA}$.